The 2014 World Congress on
Advances in Civil, Environmental, and Materials Research (ACEM14)
Busan, Korea, August 24-28, 2014

Numerical study of the flow over a circular cylinder in oscillatory flows with zero and non-zero mean velocity

*Shuyang Cao[1)], Ming Li[2)], Jinxing Cao[1)]

[1)] *State Key Lab for Disaster Reduction in Civil Engineering, Shanghai, China*
[2)] *Wuhan Bridge Science Research Institute, Wuhan, China*
[1)] *shuyang@tongji.edu.cn*

ABSTRACT

Flow past a circular cylinder in oscillating flows is of direct relevance to some structural engineering problems in which flow-induced vibration is one of the most important issues to consider. This study considers two kinds of oscillating flows with a zero-mean velocity and a non-zero-mean velocity respectively. The flow oscillates around the circular cylinder when the mean velocity is zero, but flows downstream while oscillating sinusoidally when the mean velocity does not equal to zero. The aerodynamic forces acting on a circular cylinder and the corresponding flow patterns are investigated in this study, with a focus on the effects of *KC* number and *AR* number.

1. INTRODUCTION

Vortex shedding behind two-dimensional circular cylinders has been one of the most studied subjects in the field of computational wind engineering in the past several decades because of its practical and the theoretical importance. Although a quite comprehensive understanding of the vortex dynamics in a cylinder's wake has been achieved, the simplicity of the geometry and the abundance of interesting flow features continue to make this phenomenon the subject of many current studies. This paper studies the flow past a circular cylinder in oscillating flows with zero and non-zero mean velocity. This flow configuration is chosen as study objective because it might be considered as a starting point to study the turbulence effect on bluff body aerodynamics. In mathematics, the time-dependent velocity fluctuation of turbulence can be decomposed into a set of simple oscillating functions. Present study that considers a fluctuating flow with one frequency component might help shedding light on the turbulence effect.

The sinusoidal oscillatory flow is expressed as

$$U(t) = U_0 + U_m \sin \omega t \tag{1}$$

where $\omega = \frac{2\pi}{T}$, $U(t)$ is the time-dependent velocity, U_0 is mean velocity of the flow, U_m is the amplitude of the sinusoidal velocity fluctuation, and T is the period of oscillation. The flow can be divided into two categories, one is the zero-mean velocity flow ($U_0 = 0$) and the other is non-zero-mean velocity flow ($U_0 \neq 0$). When $U_0 = 0$, the separated vortex oscillates in the flow also, resulting in complicated wake around the cylinder. Keulegan-Carpenter number ($KC = U_m T / D$) is an important parameter to categorize the wake flow pattern. Morison (1950) proposed a semi-empirical equation to estimate the force on a circular cylinder subjected to zero-mean-velocity sinusoidal oscillatory flow. Till now, there have been many studies on appropriate determination of the force coefficients in Morison's formula as well as the dependence of flow structure on the KC number and Reynolds number (Keulegan and Carpenter 1958; Sarpkaya 1975; Tatsuno and Bearman 1990). In addition to the KC number, Amplitude Ratio number ($AR = U_m / U_0$), which is the ratio of the amplitude of the sinusoidal velocity fluctuation to the mean velocity, is another important parameter in determining the flow structure. One of the focuses of past studies is whether the Morison's formula applicable to the sinusoidal oscillatory flow with a non-mean velocity (Nomura et al. 2003; Chen et al. 2009; An et al. 2011). This paper considers the unidirectional sinusoidal oscillatory conditions, i.e. $AR < 1$, in which the flow always flows downstream with an oscillating frequency component. In this study, the effects of KC and AR are mainly discussed while the effects of Reynolds number are paid attention to.

Direct Numerical Simulation (DNS) and Large Eddy Simulation (LES) are performed to study the flow around a circular cylinder subjected to sinusoidal oscillatory flow with zero-mean velocity and non-zero-mean velocity at $Re = 200$ and 1615. An open source solver OpenFOAM is utilized in this study. Time-mean and instantaneous flow structure at different KC number and AR number are studied in order to improve the understanding of wake structure. Basic parameter related to the vortex shedding such as Strouhal number, drag and lift coefficients and their dependence on KC number and AR number are presented. Applicability of Morison equation to the non-zero-mean oscillating flow is discussed also.

2. NUMERICAL METHOD

2.1 Governing equations and numerical procedure

The governing equations for Large Eddy simulation ($Re = 1615$) are the filtered continuity equation and Navier-Stokes equations:

$$\frac{\partial(\overline{u_i})}{\partial x_i} = 0 \tag{2}$$

$$\frac{\partial(\overline{u}_i)}{\partial t} + \frac{\partial(\overline{u}_i \overline{u}_j)}{\partial x_j} = -\frac{1}{\rho}\frac{\partial \overline{P}}{\partial x_i} + \nu \frac{\partial^2 \overline{u_i}}{\partial x_j \partial x_j} - \frac{\partial \tau_{ij}}{\partial x_j} \tag{3}$$

Where u_i (i=1,2,3) are the three velocity components and p , t and ν denote pressure, time and kinematic viscosity, respectively. The over-bar denotes the space filtered quantities. In LES, the grid-scale turbulence is solved while the sub-grid-scale turbulence is modeled. In present study the sub-grid stress model is dynOneEqEddy, which is offered by the solver. For Direct Numerical Simulation at $Re = 200$, there is no filter operation, and the last term on the right side of Eq.(3) is omitted.

We employed a structured grid mesh system for finite volume approximation of incompressible Navier-Stokes equations. The options offered by OpenFOAM for simulation are carefully selected in order to achieve reliable results. Second-order central difference scheme is used for the convection terms and the diffusion terms. Second-order backward difference scheme is adopted for time marching. In addition, PSIO algorithm is utilized to enhance the coupling of pressure and velocity in the numerical procedure.

2.2 Calculation domain

Fig. 1 shows an example of grid system at $Re = 1615$, whose details are summarized at Table 1. Considering the difference in spanwise structure of vortex shedding at between $Re = 200$ and $Re = 1615$ (Cao et al. 2010), the length of computational domain in spanwise direction is $7D$ at $Re = 200$, which is larger than $3.2D$ at $Re = 1615$.

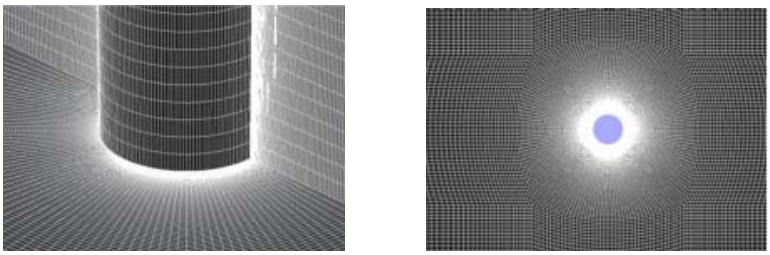

Fig.1 Example of grid system (*Re=1615*)

Table 1. Grid information

Re	Domain size	Total grids	Central region		
			Radial grid		Cir. grid
			No.	First grid	
200	$40D \times 20D \times 7D$	575,040	90	$0.006D$	112
1615	$40D \times 20D \times 3.2D$	1103520	116	$0.0025D$	160

2.3 Boundary conditions

Boundary conditions for the oscillatory flows with zero and non-zero mean velocity should be discussed, particularly at the inlet. Till now, different boundary conditions have been adopted (Dutsch et al. 1998, Iliadis and Anagnostopoulos 1998, Guilmineau and Queutey 2002, An et al. 2011). In this study, after simplifying the NS equation for the sinusoidal oscillatory flow, appropriate boundary condition for pressure is proposed at

the inlet where a sinusoidal oscillatory velocity is imposed:

$$\frac{\partial p}{\partial x} = -\rho \frac{\partial u}{\partial t} \tag{4}$$

Table 2 shows the boundary condition setup of present study, which is verified by simulating the sinusoidal oscillatory flow in an empty computational domain. Fig. 2 compares the time history of pressure and velocity at the center point of the empty computational domain between the simulation and theoretical values. Fig. 3 show the distributions of pressure and velocity in the computational domain at different phases. Both Fig. 3 and 4 are for the sinusoidal oscillatory flow with zero-mean velocity. The results for non-zero situation are not shown here. It can be found that the proposed boundary condition is suitable for the simulation of sinusoidal oscillatory flow.

Table 2 Boundary conditions

Boundary	Variable	Boundary Condition
Inlet	Speed	$u = 0.4\sin(0.4\pi t)$ (zero-mean), or $u = U_0 + U_m \sin(0.4\pi t)$ (Non-zero-mean)
	Pressure	Zero Gradient
Outlet	Speed	Pressure Inlet Outlet Velocity
	Pressure	$\frac{\partial p}{\partial x} = -\frac{0.8\pi}{5}\cos\frac{2\pi t}{5}$ (zero-mean), or $\frac{\partial p}{\partial x} = -\frac{2\pi U_m}{5}\cos\frac{2\pi t}{5}$ (non-zero-mean)

Boundary	Variable	Boundary Condition
Lateral boundaries	Speed	slip
	Pressure	Zero Gradient
Up and bottom boundaries	Speed	periodic
	Pressure	periodic

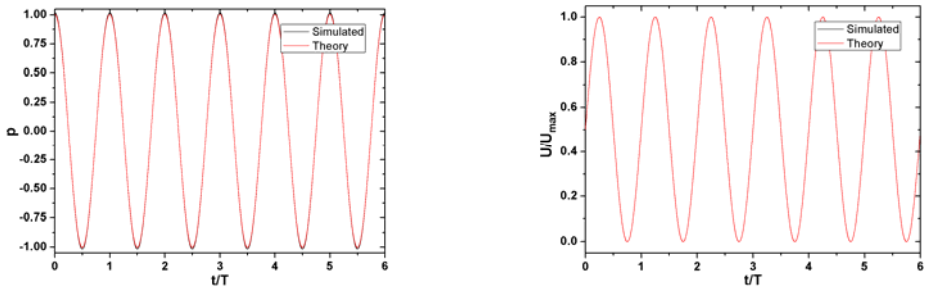

Fig.2 Comparison of the time history of pressure and velocity between the simulation and theoretical values

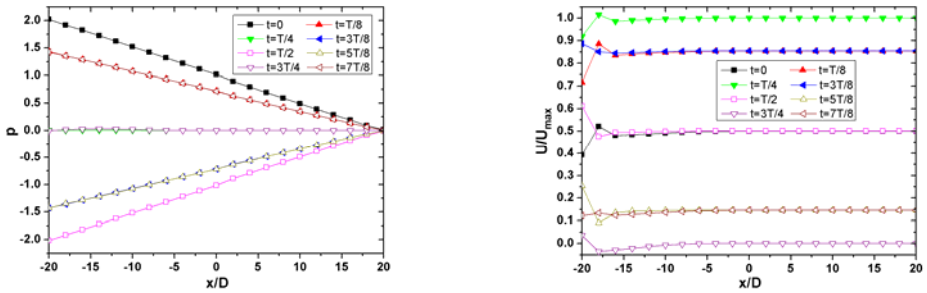

Fig.3 Distribution of pressure and velocity inside the computational domain

3. VALIDATIONS

Detailed comparison of the first- and second- order turbulence statistics on the near and far wakes is ideal for the validation. In this paper, the numerical method is validated by comparing the drag force coefficients and Strouhal number at uniform flow. The boundary conditions shown in Table 2 are adopted except for at the inlet ($u = constant$ and $p = 0$). Table 3 compares the drag force coefficients and Strouhal number at $Re = 200$ and *1615* with available data of other studies. Reasonable agreements are achieved. The comparisons of time-mean and instantaneous flow structures are also made, but the results are not shown here.

Table 3 Comparison of the drag force coefficients and Strouhal number

	$\overline{C_D}$	St		$\overline{C_D}$	St
Guilmineau(2002) ($Re = 200$)	1.286	0.195	Zdravkovich(1997) ($Re = 1000$)	1.03	
Williamson(1988) ($Re = 185$)		0.193	Norberg(2001) ($Re = 1500$)		0.212
Cao et. al ($Re = 200$)	1.300	0.186	Kravchenko (1999) ($Re = 3900$)	1.04	0.210
Present ($Re = 200$)	1.343	0.191	Present ($Re = 1615$)	1.062	0.224

4. NUMERICAL RESULTS AND DISCUSSIONS

4.1 Zero-mean-velocity oscillatory flow

As examples of zero-mean velocity oscillatory flow, two simulation cases with $KC = 10$ ($u = 0.4\sin\frac{2\pi t}{5}$) at $Re = 200$ (Case A) and $KC = 17$ ($u = 0.68\sin\frac{2\pi t}{5}$) at $Re = 1615$ (Case B) are presented. These two cases correspond to model F and model G vortex shedding, respectively, following the definition of Tatsuno (1990).

Fig. 4 depicts that a slant vortex street forms around the cylinder in oscillating flow. Two pairs of vortex (C-D and E-F) are shed during one oscillating cycle.

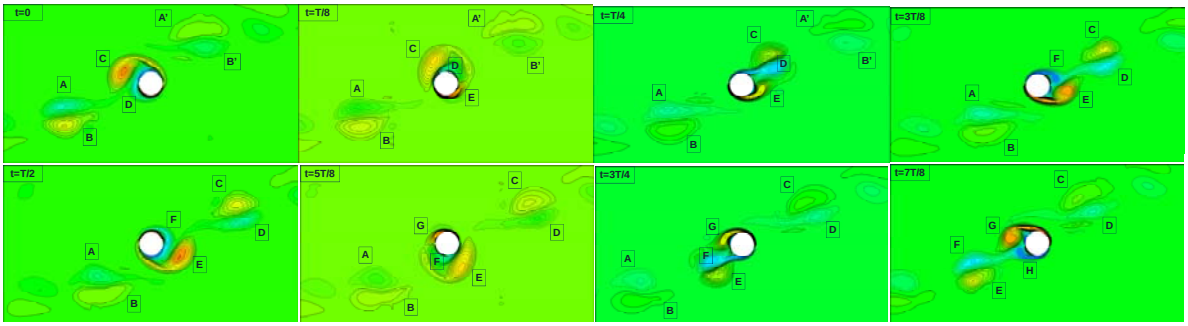

Fig.4 Instantaneous vortex structure during one oscillating cycle

Fig. 5 compares the vorticity obtained in present study with those of Dutsch (1998).

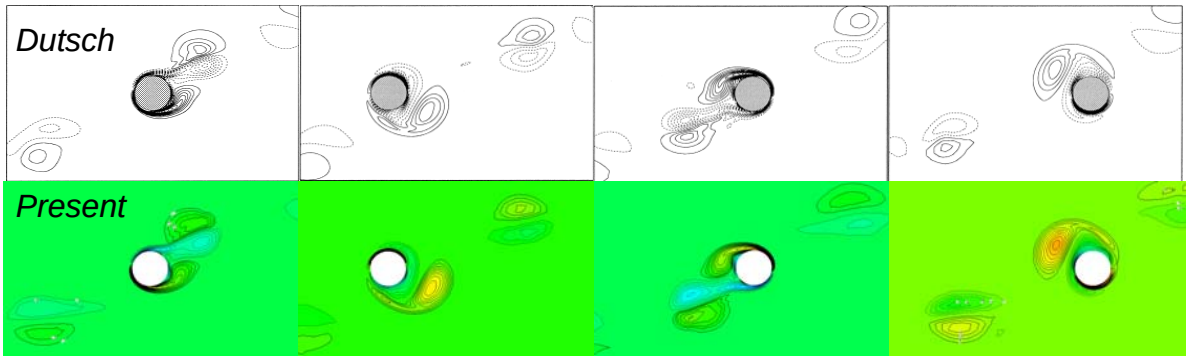

Fig. 5 Comparison of the vorticity of present study with Dutsch's result

Spectrum analysis is performed on the drag and lift force coefficients to obtain the vortex shedding frequency. As shown in Fig. 6 ($KC = 10$, $Re = 200$), the spectra of both drag and lift force coefficient exhibit several peaks at the frequencies whose values are integral times of inflow frequency. However, the inflow oscillating frequency is the dominant frequency in the drag force.

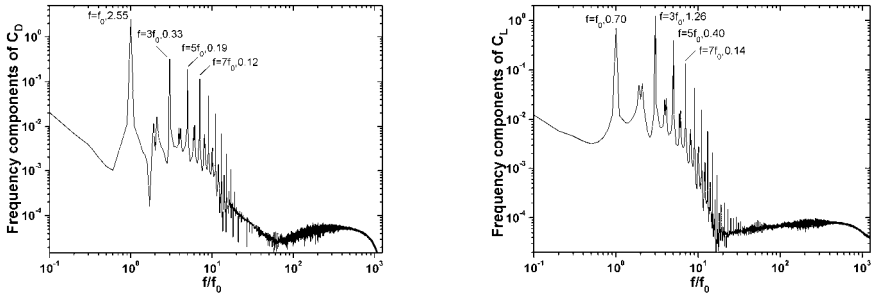

(a) Drag force coefficients (b) Lift force coefficients

Fig. 6 Power spectrum of drag and lift force coefficients

4.2 Unidirectional oscillatory flow

As examples of non-zero-mean velocity oscillatory flow, three simulation cases with

$AR = 0.2$, 0.5 and 1.0 are considered for both $Re = 200$ and 1615 at $KC = 10$. Note that a smaller AR implies that the flow is closer to non-oscillatory flow. Fig. 7 depicts the vortexes structures obtained at Re=200 and 1615 at different AR numbers.

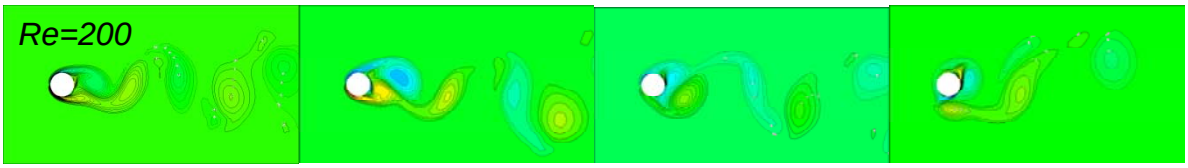

(a) AR=0 (b) AR=0.2 (c) AR=0.5 (d) AR=1.0

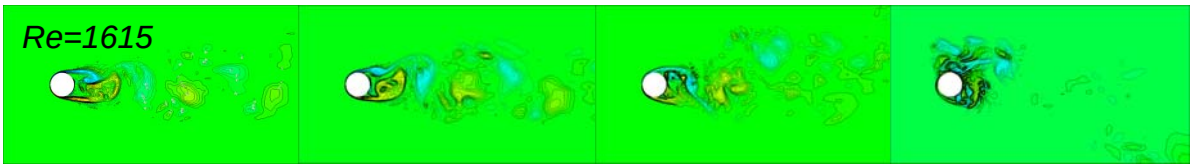

(a) AR=0 (b) AR=0.2 (c) AR=0.5 (d) *AR=1.0*

Fig. 7 Vortex structure of different AR numbers

Spectrum analysis on the drag force shows that the oscillating frequency is still dominant although several peaks co-exist as in the non-mean oscillatory flow. However, with the decrease of AR, the oscillating frequency becomes not so dominant (refer to Fig. 8a). Vortex shedding frequency appears not only at $2f_0$, $3f_0$, $4f_0$ $\cdots$, but also at $1.5f_0, 2.5f_0, 3.5f_0, \cdots$. As shown in Fig. 8b, multiple vortex shedding frequencies co-exist, and it is difficult to judge which is dominant.

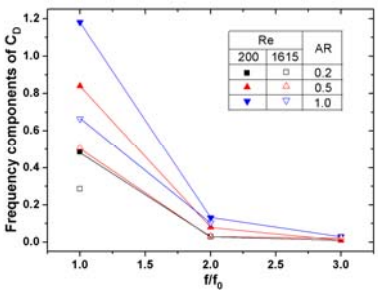

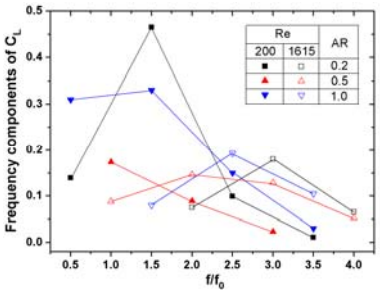

(a) Drag force (b) Lift force

Fig. 8 Comparison of amplitude of power spectra at different peak frequencies

Table 4 compares the drag and life force coefficients obtained at different AR numbers and Re numbers. When the AR number increases, the mean drag force decreases, but the RMS of drag force increases. It indicates that the pressure gradient contributes more to the drag force with increase in AR number. The variation of RMS of lift force is not consistent at two Reynolds number. The relation of this result with the vortex structure is still under investigation.

Table 4 Comparison of drag and lift force obtained at different AR

$Re = 200$	$\overline{C_D}$	C'_D	C'_L	$Re = 1615$	$\overline{C_D}$	C'_D	C'_L
$AR = 0$	1.344	0.029	0.473	$AR = 0$	1.062	0.031	0.177
$AR = 0.2$	0.978	0.343	0.351	$AR = 0.2$	0.779	0.204	0.162
$AR = 0.5$	0.626	0.596	0.182	$AR = 0.5$	0.630	0.363	0.282
$AR = 1$	0.567	0.841	0.428	$AR = 1$	0.528	0.484	0.355

5. FEASIBILITY OF MORISON EQUATION

5.1 Zero-mean-velocity oscillation flow

Morison proposed a semi-empirical equation to estimate the force on a circular cylinder subjected to zero-mean-velocity sinusoidal oscillatory flow (Morison et al. 1950). Morison formula divides the force into two parts, i.e. the drag force and inertial force:

$$F_D = \frac{1}{2}\rho B C_d |U| U + \rho A C_i \dot{U} = F_D^S + F_D^U \tag{5}$$

where the drag force coefficient C_d and inertial force coefficient C_i can be are calculated by (Keulegan and Carpenter 1958):

$$C_d = \frac{3}{4}\int_0^{2\pi} \frac{F_D \sin\theta}{\rho D U_m^2} d\theta = \frac{3}{8}\int_0^{2\pi} C_D \sin\theta d\theta \tag{6}$$

$$C_i = \frac{2U_m}{\pi^3 D}\int_0^{2\pi} \frac{F_D \cos\theta}{\rho D U_m^2} d\theta = \frac{U_m T}{\pi^3 D}\int_0^{2\pi} C_D \cos\theta d\theta \tag{7}$$

By comparing the time history of drag force estimated by Morison equation with that obtained in this study, it is found that the estimated drag history agrees the simulation result well, although some deviations are recognized.

5.2 Unidirectional oscillation flow

Morison equation is considered to be applicable to estimate the drag force in non-zero-mean oscillatory flow because the dominant frequency is still the oscillatory frequency. The inertial force coefficient could be calculated by:

$$C_i = \frac{2U_m TD}{2\pi^2 A}\int_0^{2\pi} \frac{F_D \cos\theta}{\rho D U_m^2} d\theta \tag{8}$$

However, two equations are available to calculate the drag force coefficient:

$$C_d = \frac{(U_0 + U_m)^2}{2\pi U_0 U_m}\int_0^{2\pi} C_D \sin\theta d\theta \tag{9}$$

$$\text{Or, } C_d = \frac{(U_0 + U_m)^2}{2\pi(2U_0^2 + U_m^2)} \int_0^{2\pi} C_D \sin\theta d\theta \tag{10}$$

Numerical tests are conducted to calculate C_d and C_i by three methods: 1) calculate by Eq. (8) and Eq. (9); 2) calculate from Eq. (8) and Eq. (10); and 3) the least squares fitting. Fig. 9 shows that, among the three methods, the least squares fitting methods perform best. Fig. 10 compares the values of C_d and C_i calculated by three methods. Three methods arrive at same value of C_i but different value of C_d. It indicates that Morison equation is basically only valid for predicting inertial force. Thus, it will create errors for the non-zero-mean oscillatory flow.

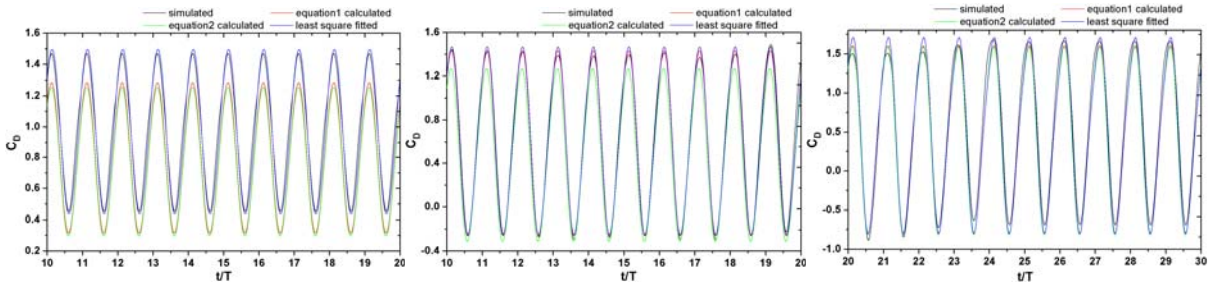

($Re = 200, AR = 0.2$) ($Re = 200, AR = 0.5$) ($Re = 200, AR = 1$)

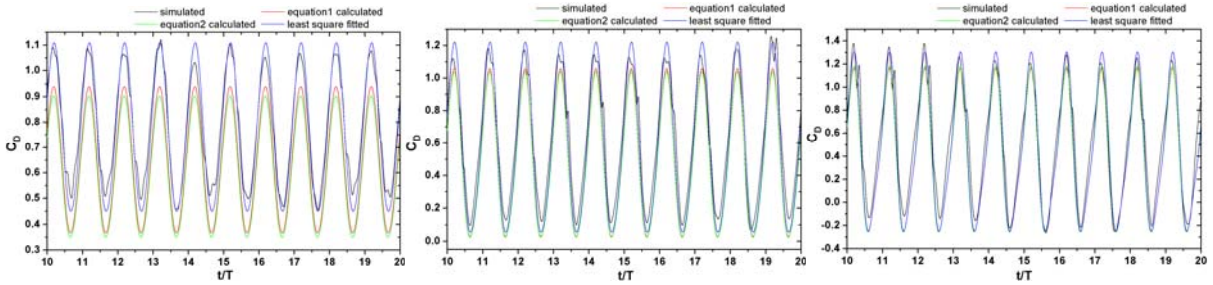

($Re = 1615, AR = 0.2$) ($Re = 1615, AR = 0.5$) ($Re = 1615, AR = 1$)

Fig. 9 Comparison of the simulated drag force

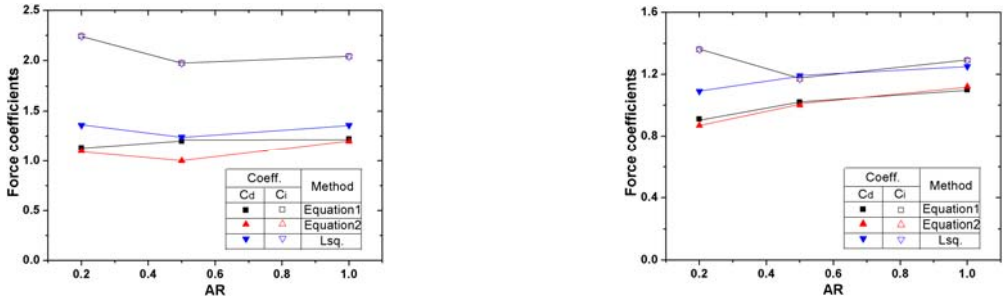

$Re = 200$ $Re = 1615$

Fig. 10 Comparison of C_d and C_i

6. CONCLUSIONS

Numerical studies of the flow over a circular cylinder in oscillatory flows with zero and non-zero mean velocity are carried out. Time-mean and instantaneous flow structure at different KC number and AR number are studied in order to improve the understanding of wake structure. Basic parameter related to the vortex shedding such as Strouhal number, drag and lift coefficients and their dependence on KC number and AR number are presented. Applicability of Morison equation to the non-zero-mean oscillating flow is checked also.

The dominant frequency on the drag force is the oscillating frequency for zero-mean flow although multi-frequency co-exists and the dominant frequency depends on AR in non-zero-mean oscillating flow. The multi-peak and dominant frequencies of lift force are dependent on the oscillating frequency and AR number.

Morison equation can be used to fitting the drag force history in both zero-mean-velocity oscillatory flow and unidirectional oscillatory flow.

ACKNOWLEDGEMENTS

This research was funded in part by Natural Science Foundation of China (NSFC) Grant No. 51278366 and National Key Basic Research 973 Program (2013CB036300) of Ministry of Science and Technology of China.

REFERENCES

Morison J.R., O'Brien M.P., Johnson J.W. and Schaaf S.A. (1950). The force exerted by surface waves on piles. Petroleum Transactions of AIME, 189, 149-154.

Keulegan G.H., Carpenter L.H. (1958). Forces on cylinders and plates in an oscillatory fluid. Journal of Research of the National Bureau of Standards, 60(5), 423-440.

Tatsuno M., Bearman P.W. (1990). A visual study of the flow around an oscillatory circular cylinder at low Keulegan-Carpenter numbers and low Stokes numbers. Journal of Fluid Mechanics, 211, 157-182.

Sarpkaya T. (1975). Forces on cylinders and spheres in a sinusoidally oscillating fluid. ASME. Journal of Applied Mechanics, 42(1), 32-37.

Nomura T., Suzuki Y., Uemura M. and Kobayashi N. (2003). Aerodynamic forces on a square cylinder in oscillating flow with mean velocity. Journal of Wind Eng. and Ind. Aerodyn., 91, 199-208.

An H.W., Cheng L. and Zhao M. (2011). Direct numerical simulation of oscillatory flow around a circular cylinder at low Keulegan-Carpenter numbers. Journal of Fluid Mechanics, 666, 77-103.

Chen C.C., Fang F.M., Li Y.C. (2009). Fluid forces on a square cylinder in oscillating flows with non-zero-mean velocities. International Journal for Numerical Methods in Fluids, 60, 79-93.

Dutsch H., Durst F., Becher S. and Lienhart H. (1998). Low Reynolds number flow around an oscillatory circular cylinder at low Keulegan-Carpenter numbers. Journal of Fluid Mechanics, 360, 249-271.

Guilmineau E. Queutey P. (2002). A numerical simulation of vortex shedding from an oscillatory circular cylinder. Journal of Fluids and Structures, 16(6), 773-794.

Iliadis G. Anagnostopoulos P. (1998). Viscous oscillatory flow around a circular cylinder at low Keulegan-Carpenter numbers and frequency parameters. International Journal for Numerical Methods in Fluids, 26, 403-442.

Cao S., Ozono S., Tamura Y., Ge Y., Kikugawa H. (2010). Numerical simulation of Reynolds number effects on velocity shear flow around a circular cylinder. Journal of Fluids and Structures, 26, 685-702.

Zdravkovich M. Flow around circular cylinders. Fundermental Vol. 1. Oxford University Press, Oxford, England, 1997.

Kravchenko A.G. and Moin P. (1999). Numerical studies of flow over a circular cylinder at ReD=3900. Physics of Fluids,12(2), 403-417.

Norberg C. (2001). Flow around a circular cylinder: aspects of fluctuating lift. Journal of Fluids and Structures, 15, 459-469.

Williamson C.H.K. (1988). Defining a universal and continuous Strouhal-Reynolds number relationship for the laminar vortex shedding of a circular cylinder. Physics of Fluids, 31(10), 2742-2744.